Extension of quasar baseline with the SDSS, PS1, and ZTF data.

Trisha Raichura

October 17, 2023

1 Introduction

1.1 What are quasars?

Quasars are the most luminous objects in our Universe. They are distant galaxies that contain an actively accelerating supermassive black hole. Quasars are seen across great cosmological distances.

Despite their immense brightness, quasars cannot be seen with the naked eye due to their distance from the Earth. It takes billions of years for the electromagnetic radiation from quasars to reach Earth's atmosphere. Therefore, the study of quasars offers astronomers crucial insights into the early phases of the universe. The term "quasar" is a shortened form of a "quasi-stellar radio source." This label was coined in the 1960s when quasars were first discovered in radio wavelengths (Matthews, Sandage, 1963). Quasar's spectral energy distribution is a broad continuum stretching from radio, to visible, to UV, X-rays, and gamma rays (Shang et al., 2011). The majority of optical emission originates from the accretion disk, which has a diameter approximately 25 times larger Hawkins (2006) than the Solar System, depending on the black hole mass (Mudd et al., 2018).

1.2 Why do we extend quasar baselines?

The quasar emission is variable at approximately 0.2 mag rms level on a timescale of months to years. The longer the observed span of the observations - the baseline - the longer the timescale of variability that can be probed. Quasar light curves in the optical-UV wavelength range can be fit with a Damped Random Walk (DRW) model, which is unbiased as long as the light curve length is greater than 10 times the DRW characteristic timescale (Kozłowski, 2017; Suberlak et al., 2021). Therefore, in this work, we extend quasar baselines with the aim of improving the fit accuracy of the DRW model.

2 Data

We use data from Panoramic Survey Telescope and Rapid Response System 1 Survey (Pan-STARRS1, PS1,Flewelling et al. 2020), Sloan Digital Sky Survey (SDSS, Annis et al. 2014) and Zwicky Transient Facility (ZTF, Bellm et al. 2018). We considered the light curves of Changing Look Quasar candidates identified by Suberlak et al. (2021), combining SDSS, PS1, and ZTF data. Each telescope records a different section of each light curve over a span of approximately 25 years (the earliest SDSS data starts in 1998, and the most recent ZTF DR17 data is from 2022). Note that each light curve appears to consist of clusters of data (see eg. Fig. 1). These correspond to epochs spaced closely in time, within a few days.

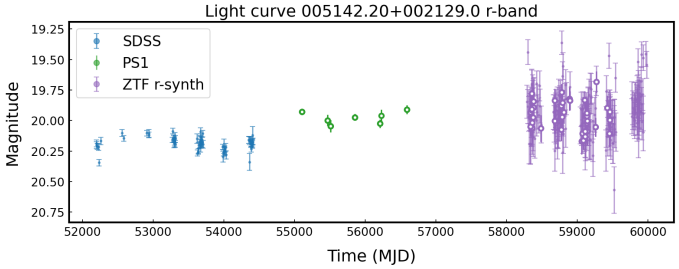

Figure 1: This figure shows the light curve for a changing look quasar candidate SDSSJ005142.20+002129.0. We show the SDSS r-band (blue), PS1 r-band (green), and ZTF r-band (purple) data. Filled dots represent individual observations, whereas open circles are day-averaged data (usually 2-5 epochs). SDSS and PS1 are shown in original photometric filters, and ZTF is shifted to the SDSS r-band using color offset (see Sec.3).

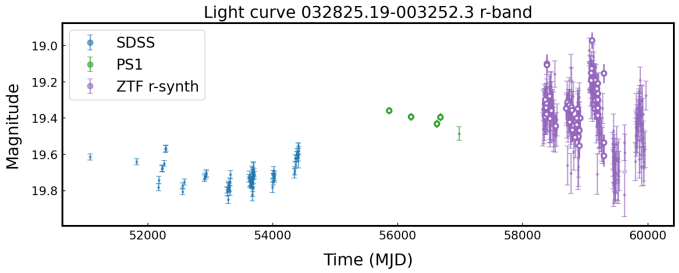

Figure 2: This figure shows the light curve for a changing look quasar candidate 032825.19-003252.3. The format of the graph in this figure corresponds to Fig.1.

3 Methods

Each dataset originates from a slightly different photometric system: SDSS-r, PS1-r[1], ZTF-r do not have identical transmissivity. See Fig. 3 for a filter comparison together with a quasar composite spectrumVanden Berk et al. (2001).

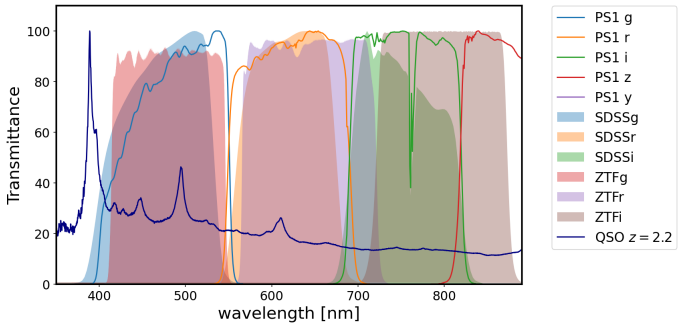

Figure 3: A composite quasar spectrum (Vanden Berk et al. 2001), with overplotted SDSS (g,r,i), ZTF (g,r,i), and PS1 (g, r, i, z, y) filter transmissivity. Note that albeit similar, the filters have different shape and spectral range. SDSS and PS1 r-bands are sufficiently similar that we are able to treat PS1 r-band as approximately equivalent to SDSS r-band (see Fig.5 in Suberlak et al. 2021). However, magnitude measurements obtained in the ZTF r-band are transformed to a synthetic version of SDSS r-band using color terms.

Given a significant difference between the SDSS-r and ZTF-r, we apply to the ZTF data color correction terms of the form

$$r_{\mathrm{SDSS,synth}} = r_{\mathrm{ZTF}} + 0.01 + 0.04(g_{\mathrm{SDSS}} - i_{\mathrm{SDSS}}) \quad (1)$$

These were derived by comparing SDSS r-band and ZTF r-band data for a subset of 40,000 SDSS standard stars (see Suberlak et al. 2021, Sec.3 for details).

Finally, we clean the combined SDSS r–PS1 r quasar light curves using standard procedures of σ-clipping in magnitude and error space and error-weighted day averaging to mitigate the impact of bad photometry and average out the intranight variability (as in Charisi et al. 2016, Suberlak et al. 2017).

4 Results

We fit the light curves with the DRW model using celerite[2] - a Gaussian Process solver (Foreman-Mackey et al. 2017, for details of the implementation see Kozłowski et al. 2010). We compare the parameters of DRW fit between using

[1] `http://panstarrs.stsci.edu`
[2] `https://celerite.readthedocs.io/en/latest/python/kernel/`

the shorter SDSS-PS1 section of each light curve (see Fig. 4) and the combined SDSS-PS1-ZTF light curve (see Fig.5). The DRW time scale τ and variability amplitude σ differ for SDSS-PS1 (Fig. 6) versus SDSS-PS1-ZTF (Fig. 7). The ZTF data extends the SDSS-PS1 portion of each light curve to MJD 58000-60000, i.e. additional 5 years. Additionally, the magnitude increases as ZTF data is added and ranges from 21.2 to some days reaching almost 19.8 whereas initially, with SDSS-PS1, there was less data collected and the magnitude varied from 21.0 to 19.9.

Time-series analysis is the application of mathematical and statistical tests to any set of time-varying data in an attempt to: 1) quantify the variation itself, and 2) use that variation to learn something about the behavior of the system. In this data, we see that when ZTF data is added to the graphs there is an increase in the time scale as well as the magnitude compared to when the graph just contained SDSS-PS1 filters(boy 2021). From this data, we can gain a physical understanding of the candidate's light curve and comprehend the cause of the timescale change. Here, after the ZTF data is compiled with SDSS-PS1 the DRW timescale becomes more increases. Each light curve is a certain prediction of the future brightness level. The larger the DRW amplitude of variability, the larger the possible departure from the current brightness level.

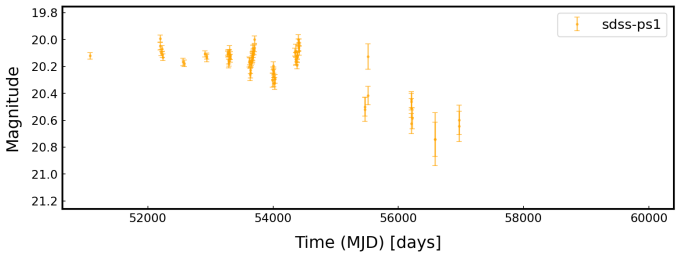

Figure 4: This figure shows only the SDSS-PS1 section of the light curve for CLQSO candidate 010812.00-000516.5.

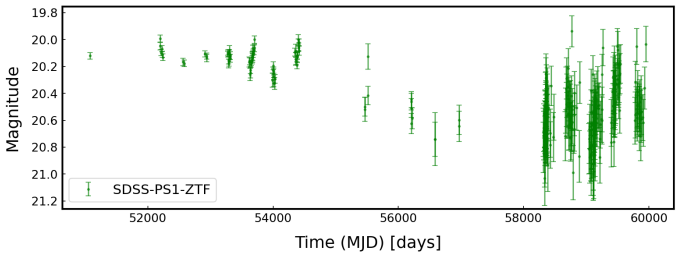

Figure 5: This figure shows the SDSS-PS1-ZTF section of the light curve for CLQSO candidate 010812.00-000516.5.

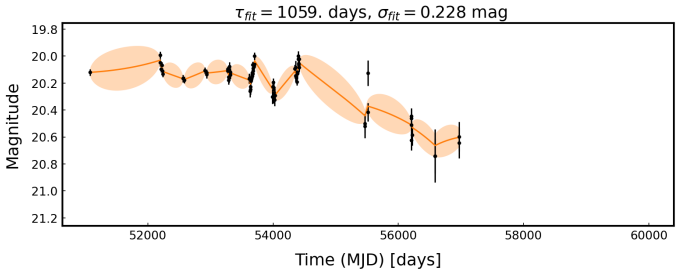

Figure 6: This figure shows the result of fitting the DRW model to the SDSS-PS1 section for CLQSO candidate 010812.00-000516.5

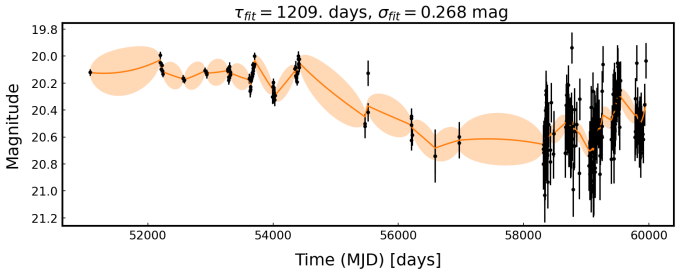

Figure 7: This DRW model fit to the SDDS-PS1-ZTF combined light curve of CLQSO candidate 010812.00-000516.5. The timescale and amplitude using a full SDSS-PS1-ZTF light curve become larger toward the days 580000-600000 when ZTF data was recorded. The rest of the data stays the same as only SDSS-PS1 were recorded on these days.

5 Summary

We have extended quasar baselines and plotted light curves with the aim of improving the accuracy of the DRW model. We used publicly available archives to combine the SDSS, PS1, and ZTF data. We employed appropriate photometric offsets (color terms) to translate between different band definitions, eg. PS1-r, ZTF-r, and SDSS-r band. We then fit CLQSO light curves with the DRW model to evaluate the impact of extending the SDSS- PS1 light curve with the ZTF data.

Adding the ZTF data to SDSS-PS1 data changes the DRW timescale and amplitude. The plot after combining with ZTF data extends the SDSS-PS1 portion of each QSO light curve to MJD 58000-60000, i.e. additional 5 years. The amplitude increases when the ZTF data is plotted and ranges from 21.2 to 19.8 whereas initially with SDSS-PS1 the magnitude varied from 21.0 to 19.9.

A Additional quasar light curves

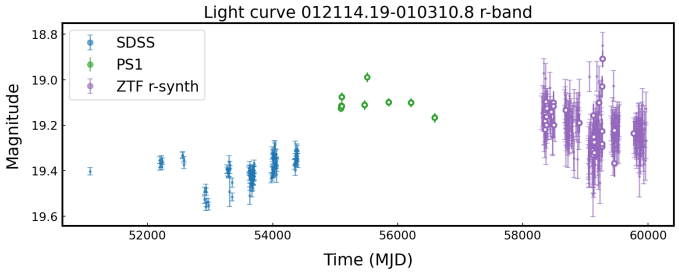

Figure 8: This figure shows the light curve for a changing look quasar candidate 012114.19-010310.8 Formatting analogous to Fig. 1.

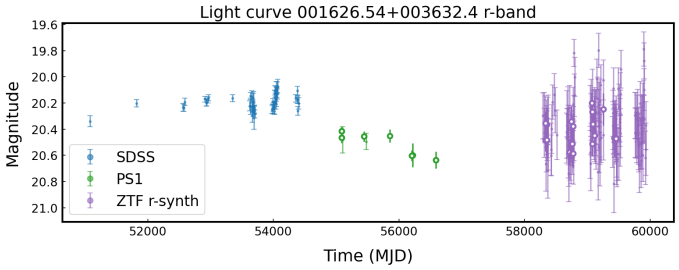

Figure 9: This figure shows the light curve for a changing look quasar candidate 001626.54+003632.4 Formatting analogous to Fig. 1.

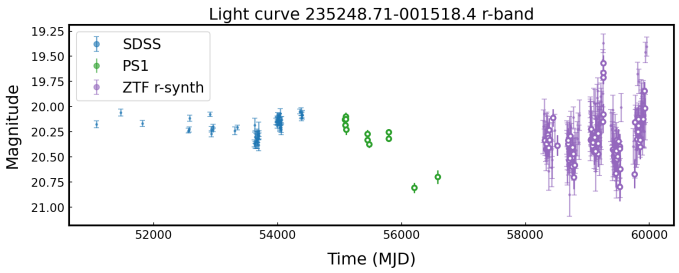

Figure 10: This figure shows the light curve for a changing look quasar candidate 235248.71-001518.4 The format of the graph in this figure corresponds to Fig. 1.

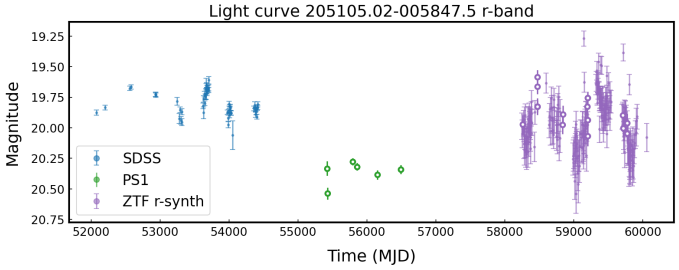

Figure 11: This figure shows the light curve for a changing look quasar candidate 205105.02-005847.5. The format of the graph in this figure corresponds to Fig. 1.

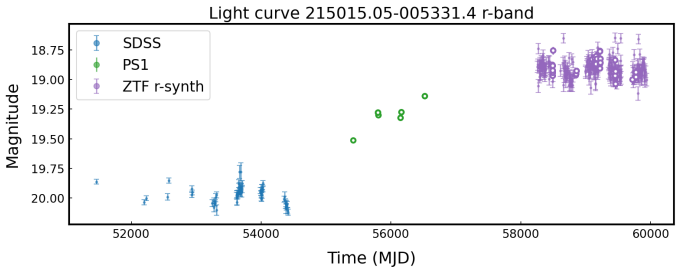

Figure 12: This figure shows the light curve for a changing look quasar candidate 215015.05-005331.4. The format of the graph in this figure corresponds to Fig. 1.

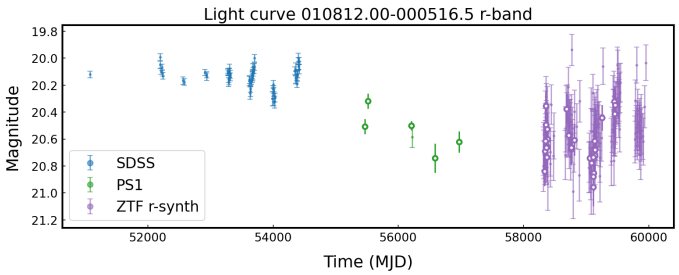

Figure 13: This figure shows the light curve for a changing look quasar candidate 010812.00-000516.5. The format of the graph in this figure corresponds to Fig. 1.

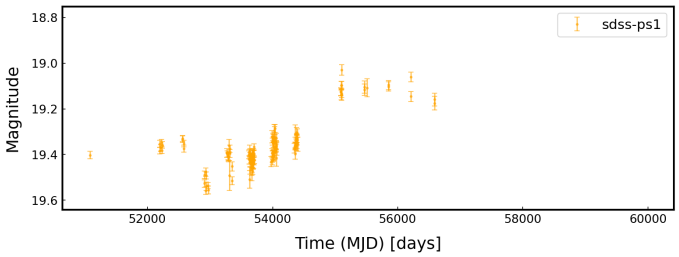

Figure 14: This figure shows only the SDSS-PS1 section of another light curve Formatting analogous to Fig. 4.

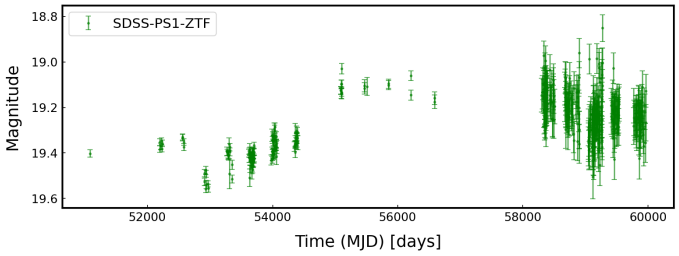

Figure 15: This figure shows the SDSS-PS1-ZTF section of the light curve Formatting analogous to Fig. 5.

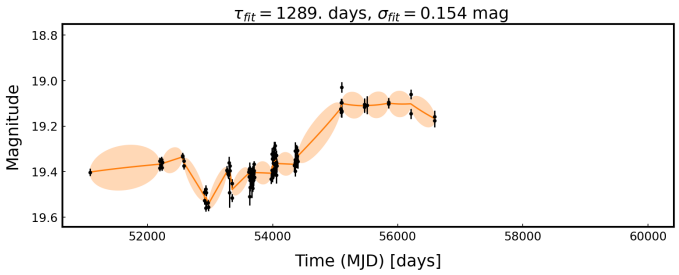

Figure 16:
Formatting analogous to Fig. 6

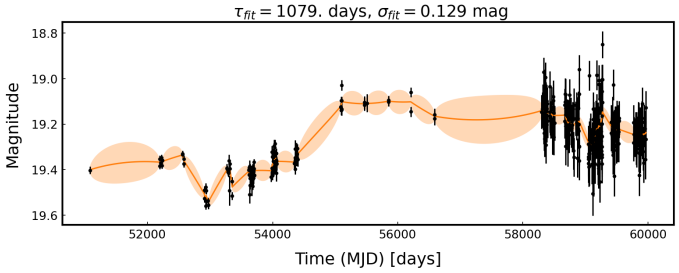

Figure 17: This DRW model fit to the SDDS-PS1-ZTF combined light curve of a CLQSO candidate

Formatting analogous to Fig. 7

References

Aug 2021.

Annis James, Soares-Santos M., Strauss Michael A, Becker A C, Dodelson Scott, Fan Xiaohui, Gunn James E, Hao Jiangang, Ivezić Željko, Jester Sebastian, Jiang Linhua, Johnston David, Kubo Jeffrey M, Lampeitl H., Lin Huan, Lupton Robert H, Miknaitis G., Seo Hee-Jong, Simet Melanie, Yanny B. THE SLOAN DIGITAL SKY SURVEY COADD: 275 deg2OF DEEP SLOAN DIGITAL SKY SURVEY IMAGING ON STRIPE 82 // The Astrophysical Journal. Sep 2014. 794, 2. 120–120.

Bellm Eric C, Kulkarni S R, Graham M J, Dekany Richard, Smith Roger M, Riddle Reed, Masci Frank J, Helou G, Prince Thomas A, Adams S M, Barbarino C, Barlow Tom A, Bauer J, Beck R, Belicki Justin, Biswas Rahul, Blagorodnova N., Bodewits Dennis, Bolin Bryce, Brinnel V. The Zwicky Transient Facility: System Overview, Performance, and First Results // Publications of the Astronomical Society of the Pacific. Dec 2018. 131, 995. 018002–018002.

Charisi M., Bartos I., Haiman Z., Price-Whelan A. M., Graham M. J., Bellm E. C., Laher R. R., Márka S. A population of short-period variable quasars from PTF as supermassive black hole binary candidates // . XII 2016. 463, 2. 2145–2171.

Flewelling H, Magnier E A, Chambers K, Heasley J N, Holmberg Conrad, Huber M E, Sweeney William E, Waters C, Calamida A., Casertano Stefano, Chen X, Farrow Daniel J, Hasinger G., Henderson Rachel E, Long Knox S, Metcalfe N, Narayan Gautham, Nieto-Santisteban Maria, Norberg Peder, Rest A. The Pan-STARRS1 Database and Data Products // Astrophysical Journal Supplement Series. Oct 2020. 251, 1. 7–7.

Foreman-Mackey D., Agol E., Ambikasaran S., Angus R. Fast and Scalable Gaussian Process Modeling with Applications to Astronomical Time Series // . XII 2017. 154. 220.

Hawkins M. R. S. Timescale of variation and the size of the accretion disc in active galactic nuclei // Astronomy Astrophysics. Nov 2006. 462, 2. 581–589.

Kozłowski Szymon. Limitations on the recovery of the true AGN variability parameters using damped random walk modeling // . I 2017. 597. A128.

Kozłowski Szymon, Kochanek Christopher S., Udalski A., Wyrzykowski Ł., Soszyński I., Szymański M. K., Kubiak M., Pietrzyński G., Szewczyk O., Ulaczyk K., Poleski R., Collaboration The OGLE. Quantifying Quasar Variability as Part of a General Approach to Classifying Continuously Varying Sources // . 2010. 708, 2. 927.

Matthews Thomas A., Sandage Allan R. Optical Identification of 3c 48, 3c 196, and 3c 286 with Stellar Objects. // The Astrophysical Journal. Jul 1963. 138. 30.

Mudd D., Martini P., Zu Y., Kochanek C., Peterson B. M., Kessler R., Davis T. M., Hoormann J. K., King A., Lidman C., Sommer N. E., Tucker B. E., Asorey J., Hinton S., Glazebrook K., Kuehn K., Lewis G., Macaulay E., Moeller A., O'Neill C., Zhang B., Abbott T. M. C., Abdalla F. B., Allam S., Banerji M., Benoit-Lévy A., Bertin E., Brooks D., Rosell A. Carnero, Carollo D., Kind M. Carrasco, Carretero J., Cunha C. E., D'Andrea C. B., Costa L. N. da, Davis C., Desai S., Doel P., Fosalba P., García-Bellido J., Gaztanaga E., Gerdes D. W., Gruen D., Gruendl R. A., Gschwend J., Gutierrez G., Hartley W. G., Honscheid K., James D. J., Kuhlmann S., Kuropatkin N., Lima M., Maia M. A. G., Marshall J. L., McMahon R. G., Menanteau F., Miquel R., Plazas A. A., Romer A. K., Sanchez E., Schindler R., Schubnell M., Smith M., Smith R. C., Soares-Santos M., Sobreira F., Suchyta E., Swanson M. E. C., Tarle G., Thomas D., Tucker D. L., Walker A. R., Collaboration DES. Quasar Accretion Disk Sizes from Continuum Reverberation Mapping from the Dark Energy Survey // The Astrophysical Journal. jul 2018. 862, 2. 123.

Shang Zhaohui, Brotherton M S, Wills Beverley J, Wills D, Cales Sabrina, Dale Daniel A, Green Richard F, Runnoe Jessie C, Nemmen R., Gallagher S C, Ganguly R, Hines Dean C, Kelly Benjamin J, Kriss G A, Li Jun, Tang Baitian, Xie Yanxia. THE NEXT GENERATION ATLAS OF QUASAR SPECTRAL ENERGY DISTRIBUTIONS FROM RADIO TO X-RAYS // Astrophysical Journal Supplement Series. Aug 2011. 196, 1. 2–2.

Suberlak K., Ivezić Ž., MacLeod C. L. Improving Damped Random Walk Parameters for SDSS Stripe 82 Quasars with Pan-STARRS1 // The Astrophysical Journal. feb 2021. 907, 2. 96.

Suberlak K., Ivezić Ž., MacLeod C. L., Graham M., Sesar B. Solving the puzzle of discrepant quasar variability on monthly time-scales implied by SDSS and CRTS data sets // . XII 2017. 472. 4870–4877.

Vanden Berk D. E., Richards G. T., Bauer A., Strauss M. A., Schneider D. P., Heckman T. M., York D. G., Hall P. B., Fan X., Knapp G. R., Anderson S. F., Annis J., Bahcall N. A., Bernardi M., Briggs J. W., Brinkmann J., Brunner R., Burles S., Carey L., Castander F. J., Connolly A. J., Crocker J. H., Csabai I., Doi M., Finkbeiner D., Friedman S., Frieman J. A., Fukugita M., Gunn J. E., Hennessy G. S., Ivezić Ž., Kent S., Kunszt P. Z., Lamb D. Q., Leger R. F., Long D. C., Loveday J., Lupton R. H., Meiksin A., Merelli A., Munn J. A., Newberg H. J., Newcomb M., Nichol R. C., Owen R., Pier J. R., Pope A., Rockosi C. M., Schlegel D. J., Siegmund W. A., Smee S., Snir Y., Stoughton C., Stubbs C., SubbaRao M., Szalay A. S., Szokoly G. P., Tremonti C., Uomoto A., Waddell P., Yanny B., Zheng W. Composite

Quasar Spectra from the Sloan Digital Sky Survey // . VIII 2001. 122. 549–564.